DESIGN OF HIGH SPEED TEST ROTORS FOR PULSE ALTERNATOR COMPONENT DEVELOPMENT

By:

M.D. Werst
J.J. Hahne
H.P. Liu
C.E. Penney

Eleventh EML Technology Symposium, Saint-Louis, France, May 14-17, 2002

Attached paper is the final version as submitted to the conference. IEEE performs final layout in-house to distribute figures and tables within the text.

PR - 310

Center for Electromechanics
The University of Texas at Austin
PRC, Mail Code R7000
Austin, TX 78712
(512) 471-4496

May 3, 2002

Design and Testing of a High Speed Spin Test for Evaluating Pulse Alternator Windage Loss Effects

Michael D. WERST, Jonathan J. HAHNE, Hsing P. LIU, and Charles E. PENNEY

***Abstract*-- Advance pulse alternator designs require rotor surface speeds in excess of 1,000 m/s. High tip speeds and an operating environment consisting of partial vacuum result in frictional windage losses and subsequent heating of the rotor and stator surfaces. Analytical models for cylindrical rotor windage loss exist. However, solving the combined fluid dynamics and thermal conduction problem for this specific operating regime requires significant code development. A series of spin tests with incremental levels of complexity have been designed and tested and are presented in this paper. The tests are intended to validate windage loss and heating codes used in the pulse alternator rotor design.**

I. Introduction

The frictional windage losses associated with the airflow in an annular air gap between the rotor and stator of a high-speed pulse alternator (or compulsator) results in torques and frictional heating. The torque must be made up by the motoring source while the heating must be considered in the design of temperature sensitive rotor and stator components. Sustaining a sufficiently low pressure to negate windage loss is impractical given the type of seals necessary for pulse alternator operation and practical vacuum pump capacities.

For a continuum flow between concentric rotating cylinders, secondary flow of rows of circumferential Taylor vortices will be formed. This is due to centrifugal flow instability of a curved flow at relatively high rotating speed. The characteristics of these air-gap flows have been of general interest in many engineering applications. In the past, many analytical and experimental investigations have been conducted to quantify the windage losses [1-5], primarily with rotor tip velocities lower than 200 m/s. The windage data for compressible supersonic air-gap airflow is generally not available.

Existing semi-empirical formulas have been used to predict high-speed pulse alternator windage losses at low cover gas pressures. Fig. 1 [6] shows predictions for windage loss vs. rpm for a hypothetical pulse alternator design with a tip speed of 1,100 m/s. The accuracies of these predictions are uncertain since they were obtained using semi-empirical formulas developed from test results with low rotor velocities. The curves also illustrate the strong windage loss dependency on vacuum level. The apparently simple solution to minimize windage losses is to reduce the operating vacuum level.

Pulse alternators utilize carbon graphite shaft seals to separate bearing lubricants from the stator cavity. These seals require a nitrogen buffer gas to allow the carbon graphite segments to seal and not overheat at the high surface speeds. Inevitably, some nitrogen gas leaks into the stator cavity. Typically, a roughing vacuum pump is used to maintain a low pressure in the stator cavity. Even with an exceptional seal surface with minimal total indicated runout (TIR), seal leakage will increase with speed. This phenomenon is evident by a gradual increase in stator cavity pressure as the rotor rpm increases. Increasing vacuum pump capacity is effective in reducing stator pressure. However, this also aggravates seal buffer gas leakage and is only practical in a laboratory setting. If a compact and fieldable pulse alternator is to be realized, pumps and other auxiliary systems must be minimized. Ultimately, the solution will be to improve the shaft seals. In addition, the effect of operating high-speed rotors in a partial vacuum must be understood.

II. Spin Test Design

A section view of the windage test rotor and stator are shown in Fig. 2. This spin test is designed to simulate pulse alternator rotor-to-stator "air-gap" conditions and, through a series of tests, attempts to characterize windage losses and associated heat distributions. The test results are intended to: (1) verify windage loss codes, (2) determine heat loss distribution, (3) determine effect of N_2 gas flow on heat distribution, and (4) provide sufficient data to develop an empirical model.

The test rotor measures approximately 43.2 cm (17 in.) diameter and 12.7 cm (5 in.) long and consists of multiple preloaded composite rings pressed onto a solid titanium hub. A steel stator structure with a composite liner surrounds the rotor and supports instrumentation. The stator is hung from a torque measuring transducer mounted on the spin pit lid. The torque sensor is mounted to a structural plate, which is in turn

Manuscript received March 15, 2002. A portion of this research was carried out under the Electric Gun Program sponsored by the U.S. Army Research Laboratory through Lockheed-Martin Missile and Fire Control under contract number 4300050944.

Authors are affiliated with The University of Texas at Austin Center for Electromechanics, Austin, Texas 78758, telephone (512) 471-4496, fax (512) 471-0781.

secured to the spin pit cover plate. The test rotor is designed to operate at 900 m/s at temperatures up to 93°C (200°F).

Fabrication and assembly of rotor, stator and instrumentation components were performed at UT-CEM. Rotor balancing and spin testing were conducted at Test Devices Inc. of Hudson, Massachusetts.

III. Rotor Design

The windage test utilizes an existing UT-CEM composite flywheel “on-loan” from the Containment IV program. The flywheel design features a solid titanium hub with eight preloaded graphite composite bandings (Fig. 3). The rotor dimensions are approximately 43.2 cm (17 in.) diameter by 12.7 cm (5 in.) long. The rotor is a drop from the small end of a rotor log from which several rotors were built. The outside surface of the rotor is tapered 0.025 cm/cm (0.025 in./in.). Pulse alternator rotors are also tapered to facilitate radial preloading during assembly. The maximum operating speed for the rotor is 40 krpm (900 m/s) and peak operating temperature is 93°C (200°F). The peak operating strain in the outer banding is approximately 1% at 40 krpm and the radial growth is 1.0 mm (0.040 in.). The rotor is attached to the spin pit turbine via a 0.95 cm (0.375 in.) diameter by a 20.3 cm (8.0 in.) quill shaft. Balancing of the rotor was accomplished by drilling holes in the titanium.

IV. Stator Design

The purpose of the stator structure in the windage spin test is to provide a close boundary surface to generate the windage “drag” or loss on the composite rotor. The main stator structure is a carbon steel tube, 0.95 cm (0.375 in.) thick wall, with a bolt flange on each end. The bore of the steel tube is machined with a 0.025 in./in. taper to match the taper of the rotor. Immediately inside the steel tube is a hoop-wound G-10 composite cylinder with an approximately 1.0 cm (0.400 in.) wall thickness. This G-10 cylinder is machined to have a line-to-line fit with the ID of the steel tube. The ID of the G-10 liner tube is also machined with a 0.025 cm/cm (0.025 in./in.) taper. The purpose of the G-10 liner tube is to closely approximate the composite ID surface of an electrical generator. Recent air core generators built and tested at UT-CEM have been designed and built with a thin composite tube on the ID of the stator for structural and insulation reasons. The G-10 liner provided a composite boundary on the stator ID to get representative heat flow into a composite layer. The ends of the stator structure are closed by bolting on a 0.95 cm (0.375 in.) thick 6061-T6 aluminum plate. The top aluminum plate has a short aluminum extension ring and a thin G-10 thermal barrier ring attached at its center. These two rings are hollow to allow the quill shaft to pass through. Attached to the top of the G-10 thermal barrier ring is a reaction torque sensor, Teledyne Engineering® #15228. The purpose of the reaction torque sensor is to provide a real time measurement of the windage drag on the rotor by measuring the torque imparted on the stator assembly. The entire stator structure hangs from the spin pit lid via a steel mounting plate. The bottom of the stator also has a short aluminum cap, which serves several functions. First, it extends the stator structure around the bottom stub shaft so pressure in the stator can be controlled. Second, it provides a radial “stop” for the rotor so if the rotor whirls during spin up, the composite rotor is kept from impacting the composite stator liner. The last functions are to provide means of injecting nitrogen gas into the stator structure and also hold a thermocouple for measuring inlet gas temperature.

Other than providing a boundary surface for the rotor to generate windage drag, the other main function of the stator is to house the instrumentation for getting the required data and results from the test. Refer to Table 1 to review data taken and instrumentation used. The instrumentation taken during the tests include: thermocouples, pressure transducers and torque sensor. The stator has 26 type-K thermocouple channels and the rotor has five infrared thermocouple channels. There are three pressure transducers distributed radial on each inside surface of the stator base plate and cover plate. These are to provide data about any pressure distribution along the faces of the rotor while it is spinning. There are also three pressure transducers placed in the G-10 liner wall to monitor the pressure in the air gap between the rotor and stator. One of these is along the rotor centerline and the other two are aligned with the end faces of the rotor.

The rotor heat input was monitored by observing the rotor surface temperature with infrared sensors. These sensors were mounted in the stator structure and were flush with the inside surface of the G-10 liner. They looked at the black OD surface of the rotor composites. This temperature profile was used to calculate the heat input to the rotor material.

V. Data Acquisition System

The instrumentation set-up includes many components. The sensors have been described previously. All of the sensors are supplied by UT-CEM. The only signal supplied by Test Devices was the speed analog signal. The acquisition part of the system is an Agilent 34970A data logger using three Agilent 34901A 20 channel interface cards. This set-up is capable of recording up to 60 channels of data; a total of 44 data channels were used. The Agilent data logger is controlled remotely using a Dell Latitude laptop computer with National Instruments GPIB card plugged into the PCMCIA slot. To extend the laptop further from the data logger, a pair of National Instruments GPIB Bus extenders were used. The bus extenders require a fiber optic duplex cable with SMA connectors to connect them together. The fiber optic cable is 30 m long, although a longer cable can be used if the test site set-up requires. Three duplex wall outlets are also provided by Test Devices.

VI. Testing

The rotor was spin tested alone to 40,000 rpm (900 m/s) to verify performance without the presence of a stator structure. Vibrations were measured at both stub shafts and were determined to be acceptable. A coast down test was performed from 40,000 rpm with the spin tank vacuum of 25 mT which is the lowest pressure that could be achieved given the number of instrumentation leads and associated virtual leaks introduced by the presence of the leads. The coast down tests were performed in an attempt to quantify turbine, damper and seal drag losses from which windage losses may be inferred.

Upon completion of the “rotor alone” tests, the stator was installed and the 44 channels of instrumentation was connected and checked-out (Fig. 4). Test Devices monitored and recorded rotor and stator vibration and displacement data. As a precaution, initial tests (tests 1-7) were performed with structural links installed between the stator and spin pit lid. The rotor run-out observed during the rotor alone tests had been less than the clearances between the rotor and stator however the rotor behavior due to the presence of the stator was still unknown. After a single instrumentation check-out test to 10,000 rpm, a full-speed test to 40,000 rpm was performed at 25 mT and the rotor was allowed to coast down to 15,000 rpm before braking pressure was applied to the air turbine. Spin pit vacuum levels were measured using calibrated thermocouple-type vacuum gages provided by Test Devices. Vacuum measurements using the “built-in” pressure transducers were found to have significant thermal dependencies and unreliable for “real-time” vacuum measurements. For this reason, tests that included the introduction of nitrogen gas flow through the air-gap were not performed during this series of tests. The pressure gages were to be used to adjust nitrogen flow rates in order to regulate the stator cavity pressure. Raw pressure data was collected with the intent to generate temperature compensating calibration curves at a later date.

To maximize the number of tests performed and minimize the time required for the test hardware to cool-down between tests, the maximum test speed was reduced from 40,000 rpm to 26,700 rpm or 620 m/s which represents a meaningful rotor tip speed. Table 2 lists the tests performed and the relevant operating conditions.

Beginning with test #8, the structural links were removed allowing the stator to be supported solely by the torque sensor. The torque sensor supports the stator to the spin pit lid via four each, 10-24 UNC screws. Torque sensor data was collected for tests #8-12 and allowed direct measurement of the stator windage torque for comparison to predictions. Table 2 includes the measured and predicted windage torque for tests 8-12. As can be seen in the table, the measured and predicted windage losses show a very good agreement. Fig. 5 shows plots of measured stator torques vs. time.

Unlike the stator torque where the torque is measured directly, rotor torque may be calculated using coast down data and subtracting drag losses from other parts of the spin test equipment. From the rotor coast down data, the total drag torque may be calculated from the product of the moment of inertial of the system and the rate of change of rotor speed. The rate of change of rotor speed was calculated by curve-fitting the coast down data and taking the derivative to avoid inherent noise of the slope of the speed curves. The total rotor drag torque is calculated for each test in which the rotor was allowed to coast down and given in Table 2. This total rotor drag torque however represents all losses including turbine windage and bearing losses, damper losses, quill shaft seal drag and rotor windage. Assuming that the turbine inertial is negligible relative to the rotor inertia of 0.6624 kg-m^2, the total drag torque of the entire rotating system without the presence of a stator and the spin pit at 25 mT was calculated to be 0.678 N-m (6.0 in.-lb) at 27,600 rpm. The inertia of the rotor was calculated using a 3-D solid modeling software and confirmed with a 1-D nested ring model which accounts for the physical properties of each rotor layer. Appling the same calculation to test #11 (w/stator and 10 T) the total rotor drag torque equates to 2.34 N-m (20.7 in.-lb). Using a crude assumption that all of the drag losses calculated for the no stator coast down test are the result of turbine, damper and seals (neglecting the no stator windage loss) then the windage loss due to the stator with the cavity at 10 T is approximately 1.69 N-m (15 in.-lb) or a factor of 2.5 times the measured stator torque. At 25 mT, the magnitude of the rotor-to-stator windage torque increases to a factor of 10. It is interesting to note however that the relative increase in rotor torque as the rotor cavity pressure increases is consistent with the increases measured and predicted for the stator torque. This observation leads to the conclusion that the data from the rotor alone coast down test represents drag forces inconsistent with the spin test condition with the stator present. Given that the test data was collected using a different data acquisition system and conducted a week prior to the installation of the stator, a number of spin pit system operating conditions may have changed thus resulting in a different system losses.

VII. Conclusions

A windage test consisting of a 900 m/s rotor has been designed and tested. Direct measurements of windage drag were made using a stator torque sensor. The stator torques show very good agreement with predictions. Rotor torques were calculated using coast down data. Relative changes in rotor torque calculations are consistent with those measured and predicted for the stator. The absolute rotor torque measurements require tighter control of spin pit system operating conditions and/or detailed knowledge of the auxiliary spin pit system losses. With validation of rotor and stator torque predictions, temperature measurements performed during the spin tests of the rotor and stator will be used to develop empirical models for predicting operating temperatures in similar rotating equipment.

REFERENCES

[1] C. Gazley, "Heat Transfer Characteristics of the Rotational and Axial Flow Between Concentric Cylinders," *ASME Transactions*, pp. 79-90, January 1958.

[2] J. E. Vrancik, "Prediction of Windage Power Loss in Alternators," *NASA Technical Note D-4849*, October 1968.

[3] H. Zimmermann, A. Firsching, G. H. Dibelius, and M. Ziemann, "Friction Losses and Flow Distribution for Rotating Disks With Shielded and Protruding Bolts," *ASME Transactions, Journal of Engineering for Gas Turbines and Power*, vol. 108, pp. 547-552, July 1986.

[4] P. M. Wild, N. Djilali, and G. W. Vickers, "Experimental and Computational Assessment of Windage Losses in Rotating Machinery," *ASME Transactions, Journal of Fluids Engineering*, vol. 118, pp. 116-122, March 1996.

[5] M. Himes and J. J. Schauer, "Measurement of Heat Transfer in a Switched Reluctance Generator," *Seventh AIAA/ASME Joint Thermophysics and Heat Transfer Conference*, Albuquerque, New Mexico, June 15-18, 1998.

[6] *Fluid Flow Data Book*, Genium Publishing Corporation, New York, 1994.

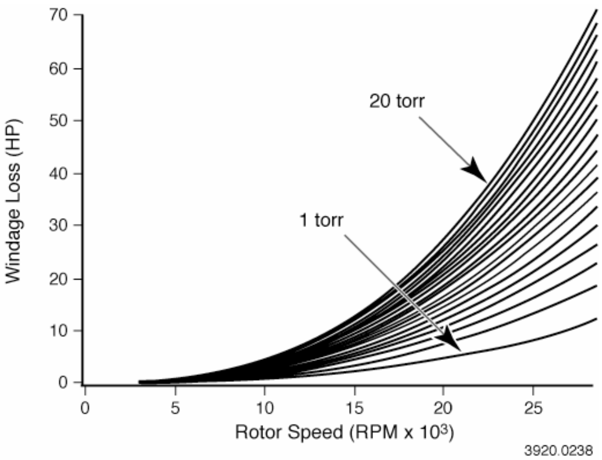

Fig. 1. Family of predicted windage loss curves vs. rotor speed for several stator cavity vacuum levels for a hypothetical rotating machine.

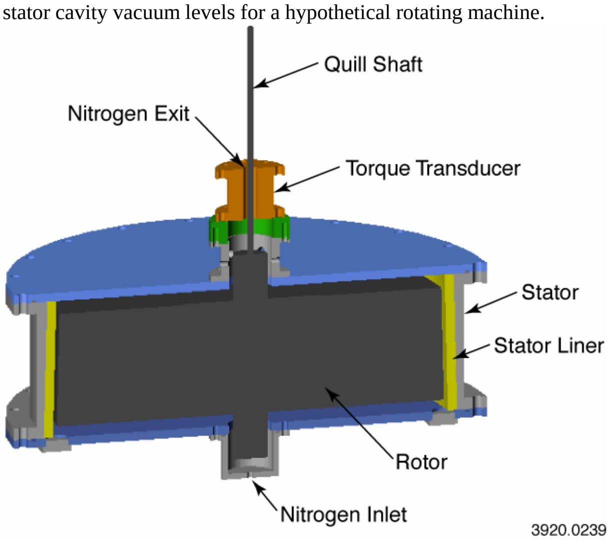

Fig. 2. Section view of windage experiment test hardware

Fig. 3. Completed 900 m/s, composite windage test rotor prior to quill shaft installation

Figure 4. Windage test hardware hung from spin pit lid

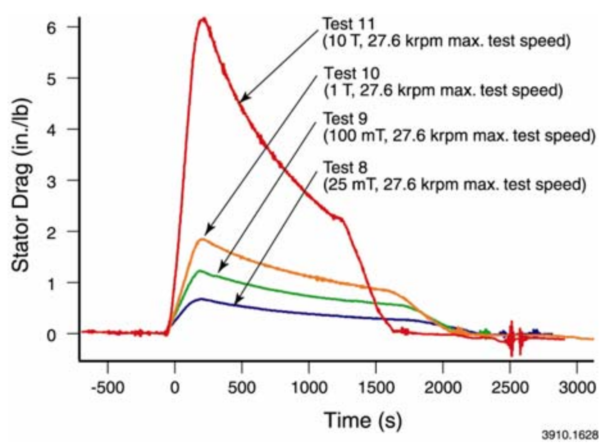

Figure 5. Measured stator torque data for tests 8, 9, 10, and 11

TABLE 1
WINDAGE HEATING SPIN TEST INSTRUMENTATION

Sensor Type	Vendor	Model #	# of Channels
Thermocouples	Omega Engineering	SA1-K	24
Pressure transducers	Advanced Custom Sensors	7201	9
Infrared sensors	Omega Engineering	0536-K-140 F	5
Torque sensor	Teledyne Brown Engineering	15228	1
N2 flowmeter	Honeywell	AWM720P1	1
N2 thermocouple probe	Omega Engineering	TJ36-CASS-14E-4	2
Power supply voltage	n/a	n/a	1
Speed (rpm)	Test Devices Provided Signal	n/a	1
		Total	44

TABLE 2
SUMMARY OF WINDAGE TEST RESULTS

Test No.	Max rpm (m/s)	Avg Tip Speed (m/s)	Time At Speed (min)	Spin Pit Vacuum (T)	Max Rotor Temp Rise (C)	Max Stator Temp Rise (ºC)	Measured Peak Torque (in.-lb)	Predicted Torque (in.-lb)	Coast Down Time * (s)	Peak Rotor System Drag Torque ** (in.-lb)
1	10,000	10,000	0	0.035	n/a	n/a	n/a	n/a	n/a	n/a
2	40,000	900	0	0.035	39	49	n/a	n/a	2,848	24.4
3	40,000	900	0	0.025	39	49	n/a	n/a	2,622	20.7
4	27,600	620	30	0.025	20	43	n/a	n/a	1,598	12.8
5	27,600	620	30	0.10	37	85	n/a	n/a	1,517	12.8
6	27,600	620	15	1	33	76	n/a	n/a	1,345	14.1
7	27,600	620	0	20	40	110	n/a	n/a	786	24.9
8	27,600	620	0	0.025	6	20	0.682	0.680	1,490	12.8
9	27,600	620	0	0.10	12	35	1.232	1.136	1,442	13.2
10	27,600	620	0	1	15	40	1.876	1.793	1,335	14.3
11	27,600	620	0	10	35	89	6.150	5.684	959	20.7
12	27,600	620	270	0.020	61	96	0.612	0.602	n/a	n/a

*Coast down time is from maximum speed to 15,000 rpm **Includes drag from turbine, damper, seals and rotor windage